N-acetyl cysteine alleviates oxidative stress and protects mice from dilated cardiomyopathy caused by mutations in nuclear A-type lamins gene

Blanca Morales Rodriguez, Lara Khouzami, Valérie Decostre, Shaida Varnous, Vanja Pekovic-Vaughan, Christopher J Hutchison, Françoise Pecker, Gisele Bonne, Antoine Muchir

N-acetyl cysteine alleviates oxidative stress and protects mice from dilated cardiomyopathy caused by mutations in nuclear A-type lamins gene

Blanca Morales Rodriguez[1,2,#], Lara Khouzami[3,#], Valérie Decostre[1], Shaida Varnous[1,+], Vanja Pekovic-Vaughan[4], Christopher J. Hutchison[5], Françoise Pecker[3], Gisèle Bonne[1,#] and Antoine Muchir[1,*,#]

[1]Sorbonne Université, UPMC Paris 06, INSERM UMRS974, Center of Research in Myology, Institut de Myologie, Paris, France, [2]Sanofi R&D, Chilly-Mazarin, France, [3]Université Paris Est Créteil, Inserm UMRS 955, IMRB, Créteil, France, [4]Institute of Ageing and Chronic Disease, William Henry Duncan Building, University of Liverpool, UK and [5]Chancellery Building, Murdoch University, Australia

*To whom correspondence should be addressed at: Center of Research in Myology, Institut de Myologie, Sorbonne Université, UPMC Paris 06, INSERM UMRS974, Paris, France. Email: a.muchir@institut-myologie.org

Abstract

Cardiomyopathy caused by lamin A/C gene (*LMNA*) mutations (hereafter referred as *LMNA* cardiomyopathy) is an anatomic and pathologic condition associated with muscular and electrical dysfunction of the heart, often leading to heart failure-related disability. There is currently no specific therapy available for patients that target the molecular pathophysiology of *LMNA* cardiomyopathy. We showed here an increase in oxidative stress levels in the hearts of mice carrying *LMNA* mutation, associated with a decrease of the key cellular antioxidant glutathione (GHS). Oral administration of N-acetyl cysteine, a GHS precursor, led to a marked improvement of GHS content, a decrease in oxidative stress markers including protein carbonyls and an improvement of left ventricular structure and function in a model of *LMNA* cardiomyopathy. Collectively, our novel results provide therapeutic insights into *LMNA* cardiomyopathy.

Introduction

Dominant mutations in the gene-encoding nuclear A-type lamins (*LMNA*) cause dilated cardiomyopathy with conduction system disease (*LMNA* cardiomyopathy) (1,2). *LMNA* cardiomyopathy is characterized by conduction defects, arrhythmias, left ventricular dysfunction and dilation, often leading to heart failure-related disability (3–5). *LMNA* cardiomyopathy can be associated with muscular dystrophy [Emery–Dreifuss muscular dystrophy (EDMD) and the limb-girdle muscular dystrophy type 1B (LGMD1B)] (5). The management of the cardiac disease consists in controlling arrhythmia and conduction defects by implantation of a defibrillator as patients are at high risk of sudden cardiac death (3). This limits the progression of heart failure, but eventually patients require heart transplantation. There are currently no effective approaches to treat *LMNA* cardiomyopathy in the clinic. Thus, it is of great importance

+Present address: Cardiac and Thoracic Surgery Department, Cardiology Institute, Pitié-Salpêtrière University Hospital, Paris, France.
#These authors contributed equally to the work.

Received: May 4, 2018. **Revised:** June 11, 2018. **Accepted:** June 26, 2018

to clarify its molecular mechanisms and to search for potential compound to provide protection against *LMNA* cardiomyopathy.

In order to study the pathophysiology of *LMNA* cardiomyopathy and to test possible therapeutics, we have developed a mouse model carrying a missense *LMNA* mutation, leading to the substitution of the histidine 222 by a proline (H222P), identified in a family with *LMNA* cardiomyopathy (6). Homozygous mutant (*Lmna*$^{H222P/H222P}$) mice develop cardiac left ventricular dilation and systolic dysfunction and have a reduced life expectancy. We previously identified and studied multiple mechanisms that contribute, in part, to the pathophysiology of *LMNA* cardiomyopathy. These include abnormal regulation of the mitogen-activated protein kinase (MAPK) signaling cascade (7,8), altered Wnt/β-catenin signaling (9), fibrosis (10), AKT/mammalian target of rapamycin (AKT/mTOR) signaling (11) and calcium handling (12). All these signaling mechanisms have been targeted with small-molecule inhibitors in *Lmna*$^{H222P/H222P}$ mice, and all of these interventions have had some beneficial impact. However, targeting signaling of each of these pathways alone is not curative (13).

Searching for alternative ways to slow down the cardiac disease progression, we here examined the involvement of oxidative stress in the progression of the cardiac disease in *Lmna*$^{H222P/H222P}$ mice. Recent data point to a relationship between lamin mutations and altered reactive oxygen species (ROS) metabolism (14). ROS are small, short-lived signaling molecules that mediate various cellular responses (15). Excessive accumulation of ROS can lead to DNA damage and the build up of oxidized proteins and lipids. The major intracellular sources of ROS are the mitochondria and the nicotinamide adenine dinucleotide phosphate (NADPH) oxidases (NOXs). To counter the potential damaging effects of ROS, cells have evolved several antioxidant systems, including ROS-alleviating enzymes like catalase and glutathione (GSH) peroxidase (GPX) and nonenzymatic systems comprising GHS.

Herein, we show that the cardiomyopathy in *Lmna*$^{H222P/H222P}$ mice is associated with altered oxidative stress levels and GSH deficiency. Accordingly, GSH replenishment with N-acetyl cysteine (NAC) treatment reduces cardiac oxidative stress injury and ameliorates contractile dysfunction in *Lmna*$^{H222P/H222P}$ mice.

Results

Lmna$^{H222P/H222P}$ mice with cardiac dilatation display increased oxidative stress markers

To explore the role of oxidative stress pathway in the development of dilated cardiomyopathy, we studied a mouse model that present a *Lmna* mutation substituting the histidine in position 222 into a proline (6). The male mice develop a progressive contractile dysfunction and cardiac remodeling and die by 32–34 weeks of age. Similar features were observed in female *Lmna*$^{H222P/H222P}$ mice but with a later onset (6). *Lmna* p.H222P corresponds to a human disease-causing mutation associated with dilated cardiomyopathy (16). Given that a consequence of altered ROS metabolism would lead to an aberrant cardiac oxidative stress (Fig. 1A), we first assessed the steady-state cardiac protein carbonylation level in *Lmna*$^{H222P/H222P}$ mice. We showed that the protein carbonylation content was increased in hearts from *Lmna*$^{H222P/H222P}$ mice compared to WT mice, when the left ventricular function was altered at 6 months of age (symptomatic) (Fig. 1B).

Since oxidative stress can be triggered by activation of (NOXs), we examined NOX2 expression in the hearts of 6-month-old *Lmna*$^{H222P/H222P}$ mice. We observed an increased NOX2 protein and mRNA expressions in hearts from *Lmna*$^{H222P/H222P}$ mice compared to WT mice (Fig. 1C and D). We also examined expression of the antioxidant GPX enzyme 1 (GPX1) involved in the detoxification of hydrogen peroxide and lipid peroxide. We showed that GPX1 expression was decreased in hearts from *Lmna*$^{H222P/H222P}$ mice compared to WT mice (Fig. 1C). Taken together these results showed that oxidative stress was increased in *LMNA* cardiomyopathy, which is associated with reduced antioxidant protection.

NAC improves cardiac redox homeostasis in *Lmna*$^{H222P/H222P}$ mice

Given that antioxidant defense was reduced in the heart from *Lmna*$^{H222P/H222P}$ mice, we tested whether the antioxidant NAC, a GSH precursor, could delay the development of left ventricular dysfunction. *Lmna*$^{H222P/H222P}$ mice were treated with NAC (140 mg/kg per day), starting at 6 months of age for a4-week duration (Fig. 2A). We observed that the increased protein carbonylation content was decreased in hearts from NAC-treated *Lmna*$^{H222P/H222P}$ mice compared to vehicle-treated mice (Fig. 2B). Next, we showed that the level of key antioxidant GSH was lowered in *Lmna*$^{H222P/H222P}$ mice compared to WT mice, which became increased after NAC treatment, both in serum (Fig. 2C) and the hearts (Fig. 2D). We also studied the expression of two mRNA-encoding enzymes controlling GSH metabolism. *Gclc* mRNA, encoding glutamate-L-cysteine ligase, a rate-limiting enzyme in GSH synthesis, and *GsR* mRNA, encoding GSH reductase, important for maintaining GSH in a reduced state, were both upregulated by 2- and 13.7-fold, respectively, in the hearts of *Lmna*$^{H222P/H222P}$ mice (Fig. 2E). This suggests an increased expression of GSH genes as an adaptive response to counteract an increased oxidative stress in the hearts of *Lmna*$^{H222P/H222P}$ mice. However, we cannot rule out that other mechanisms are acting in the pathogenesis of *LMNA* cardiomyopathy, including a larger alteration of the antioxidant signaling. Moreover, NAC treatment decreased significantly the expression of both *Glclc* and *GsR* mRNAs in the hearts of *Lmna*$^{H222P/H222P}$ mice. These results show that NAC treatment is able to restore altered redox homeostasis in *LMNA* cardiomyopathy.

NAC improves cardiac structure and function and ameliorates fibrosis in *Lmna*$^{H222P/H222P}$ mice

Cardiac structure and function were then assessed by echocardiography before and after 1 month of NAC treatment in different groups of mice. After the treatment, heart size and left ventricular dilatation were reduced in NAC-treated *Lmna*$^{H222P/H222P}$ mice compared with vehicle-treated *Lmna*$^{H222P/H222P}$ mice (Fig. 3A). Compared with the vehicle-treated *Lmna*$^{H222P/H222P}$ mice, the NAC-treated *Lmna*$^{H222P/H222P}$ mice had significantly decreased left ventricular mass and left ventricular end systolic diameter (Table 1). NAC treatment showed a beneficial effect on fractional shortening (FS), in *Lmna*$^{H222P/H222P}$ mice compared to vehicle-treated *Lmna*$^{H222P/H222P}$ mice (Table 1). In addition, we observed a significant benefit of the delta FS changes from baseline (ΔFS) in NAC-treated *Lmna*$^{H222P/H222P}$ mice compared to vehicle-treated *Lmna*$^{H222P/H222P}$ mice (Fig. 3B). Hence, treatment with NAC for 1 month delayed the development of left ventricular dilatation and cardiac contractile dysfunction in *Lmna*$^{H222P/H222P}$ mice. It would be of interest to assess the role of NAC treatment over a longer period on the cardiac function, as well as on the survival of *Lmna*$^{H222P/H222P}$ mice.

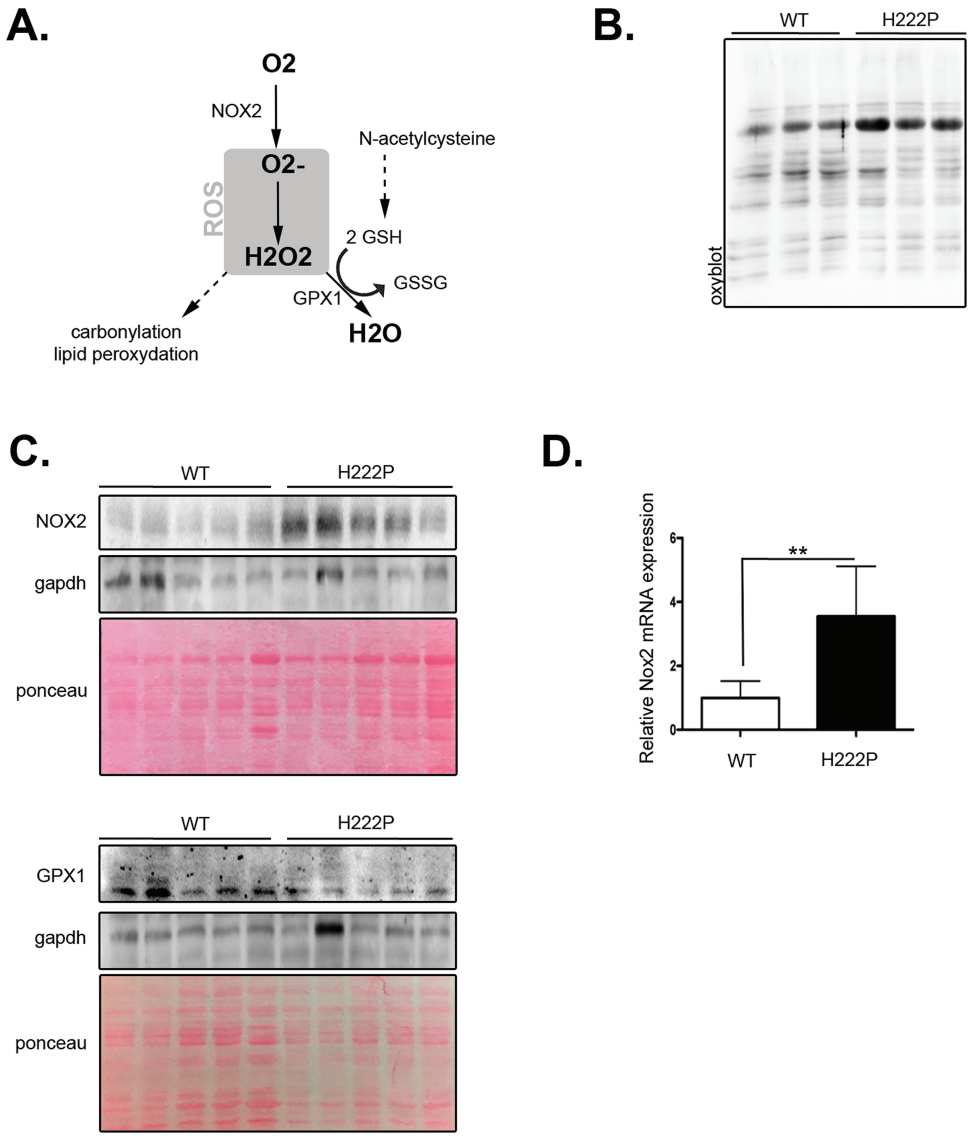

Figure 1. ROS pathway is altered in *LMNA* cardiomyopathy. (**A**) Schematic representation of the ROS pathway and consequences. (**B**) Immunoblots showing total carbonylated protein level expression (Oxyblot) in hearts from 6-month-old WT (n = 3) and from 6-month-old $Lmna^{H222P/H222P}$ (H222P) (n = 3) mice. (**C**) Immunoblots showing NOX2 and GPX1 protein level in hearts from 6-month-old WT (n = 5) and $Lmna^{H222P/H222P}$ (H222P) (n = 5) mice. Gapdh and Ponceau Red are shown as loading controls. (**D**) Expression of *Nox2* mRNA in the hearts from 6-month-old $Lmna^{H222P/H222P}$ mice (H222P) (n = 5) and WT (n = 6). Data are normally distributed and represented as means ± SEM (**P-value ≤ 0.01: P-value obtained using a two-sided Student t-test on delta Ct values).

We next hypothesized that reducing oxidative stress in the hearts of $Lmna^{H222P/H222P}$ mice would reduce myocardial fibrosis. Indeed, there was a significant reduction of myocardial fibrosis in the hearts from $Lmna^{H222P/H222P}$ mice treated with NAC relative to vehicle-treated $Lmna^{H222P/H222P}$ mice (Fig. 4A and B), as evidenced by Sirius Red staining of heart sections. All together, these results show that NAC treatment ameliorates cardiac structural and functional defects in *LMNA* cardiomyopathy, which is concomitant with restoring cardiac redox balance and antioxidant regulation.

Discussion

Our current findings indicate that *LMNA* cardiomyopathy is associated with increased oxidative stress and antioxidant GSH depletion. One-month oral NAC treatment, a GSH precursor, normalized these attributes of the cardiac disease and ameliorated the worsening of cardiac dilation and contractile dysfunction in symptomatic $Lmna^{H222P/H222P}$ mice. Based on our findings in heart, we need to further assess if abnormal oxidative stress is similarly involved in the pathogenesis of skeletal muscular dystrophy in the $Lmna^{H222P/H222P}$ mouse model of EDMD and if NAC treatment would be beneficial for the skeletal muscle structure and function.

There is a growing evidence that oxidative stress is linked to *LMNA* mutations (17,18). The precise development of oxidative stress ensuing from *LMNA* mutations still remains unknown. It has been well established that an accumulation of ROS is a direct cause of oxidative stress producing lipid peroxidation, DNA and protein oxidative damage and the loss of cells in cardiac diseases (18–20). The implications of oxidative damage and antioxidant therapy in cardiac diseases were previously studied (21–24), but this is the first demonstration of an antioxidant therapy directed toward *LMNA* cardiomyopathy.

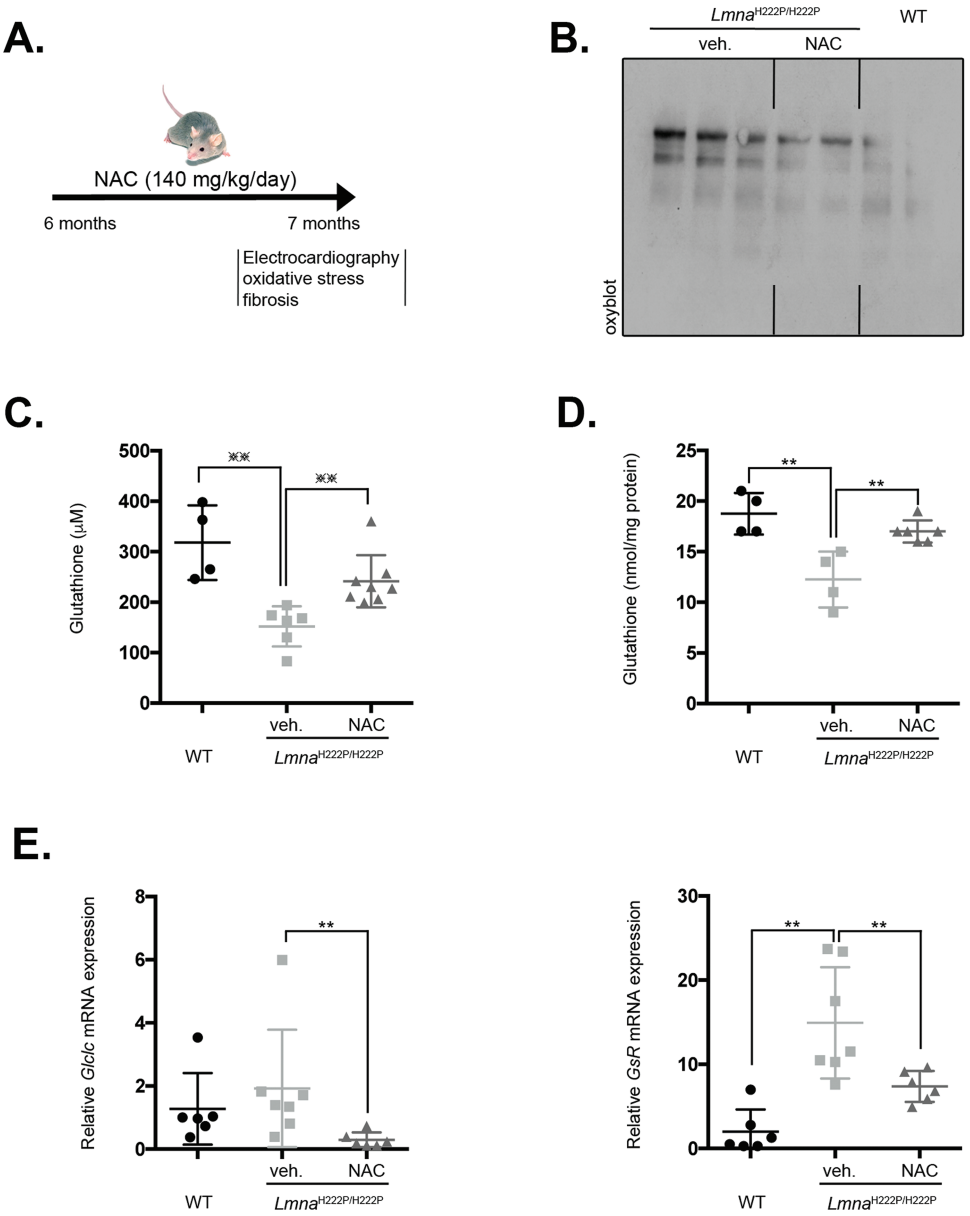

Figure 2. NAC decreases oxidative stress in *LMNA* cardiomyopathy. (**A**) Schematic representation of the treatment protocol of *Lmna*$^{H222P/H222P}$ (H222P) mice with NAC. (**B**) Immunoblots showing total carbonylated protein level expression (Oxyblot) in hearts from 7-month-old WT (n = 2) and from 7-month-old *Lmna*$^{H222P/H222P}$ (H222P) mice treated with NAC (n = 2) or vehicle (n = 2). Graph showing total GHS level in sera (**C**) and heart (**D**) from 7-month-old *Lmna*$^{H222P/H222P}$ (H222P) mice treated with NAC (n = 8 in sera and n=6 in heart) or vehicle (n = 6 in sera and n = 4 in heart). WT mice (n = 4 in sera and n = 4 in heart) are shown as control. Data are represented as median [Q1; Q3] for Figure C and as means ± SEM for D E F. Total GHS level in serum was not normally distributed, then a Wilcoxon test was performed for this parameter; all other parameters were normally distributed, then a Student t-test was performed for these parameters. (¤¤P-value ≤ 0.01: P-value obtained using a two-sided Wilcoxon test. **P-value ≤ 0.01: P-value obtained using a Student t-test). Quantitative real time PCR analysis of *Glclc* (**E**) and *GsR* mRNA expression, in 7-month-old WT mice (n = 6), *Lmna*$^{H222P/H222P}$ (H222P) mice treated with NAC (n = 6) or vehicle (n = 7). Data are represented as means ± SEM (**P-value ≤ 0.01: P-value obtained using a Student t-test on delta Ct values).

How oxidative stress results in cardiac tissue injury in *LMNA* cardiomyopathy is yet to be fully elucidated, but inference can be made from a number of related experimental studies. Evidence has linked lamins dysfunction with increased generation of ROS and reduced levels of antioxidant enzymes (25). Persistent ROS can oxidize selective cysteine residues in lamins, causing alterations in the structure of the nuclear lamina (26). The accumulation of ROS could play a role in the increased levels of DNA damage and the genomic instability observed in diseases related to mutation in *LMNA*. This notion is supported by the fact that treatment of cells expressing mutated lamins with NAC reduces the amount of unrepairable DNA damage (25). In the context of diseases caused by *LMNA* mutations, ROS have been linked with DNA damage (25,26). DNA double-strand breaks, induced by ROS, appear not to be repaired properly in cells expressing mutated lamins (27). Recent studies have shown that *Lmna* null cells exhibit signs of genomic instability and unrepaired DNA (27). These data indicate that A-type lamins deficiency affects the ability of cells to properly repair DNA damage and maintain genome integrity. Thus, compounds that reduce the levels of ROS in the cell could represent another strategy to reduce genomic instability in lamin-related diseases.

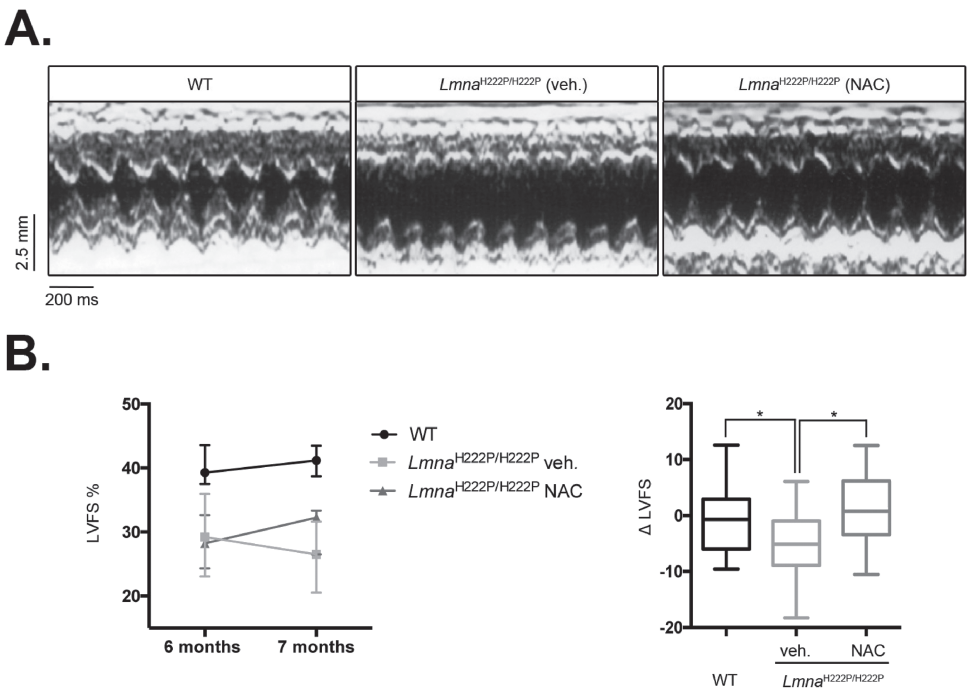

Figure 3. NAC improves cardiac structure and function in *LMNA* cardiomyopathy. (**A**) M-mode echocardiography recording at 7 months of age in WT, vehicle-treated $Lmna^{H222P/H222P}$ (H222P) and NAC-treated $Lmna^{H222P/H222P}$ mice. (**B**) Fractional shortening evolution from 6 months to 7 months from WT (n = 12), vehicle-treated $Lmna^{H222P/H222P}$ (H222P) (n = 19) and NAC-treated $Lmna^{H222P/H222P}$ mice (n = 20). ΔLVFS changes from baseline is calculated as [FS at 7 months – FS at 6 months] for each mice. Data are normally distributed and are represented as median [Q1;Q3]. (*P-value ≤ 0.05: P-value obtained using a two-sided Student t-test).

Table 1. Echocardiographic parameters for $Lmna^{H222P/H222P}$ mice treated with NAC at 7 months of age, after 1 month treatment.

Genotype	**WT**	**H222P**	**WT**	**H222P**	**H222P**
Age	**6**	**6**	**7**	**7**	**7**
Treatment	**none**	**none**	**none**	**vehicle-treated**	**NAC**
n	**12**	**39**	**12**	**19**	**20**
Heart rate (bpm)	**523.3** [509,9;536,9]	**521.7** [497.9;553,0]	**529.5** [499,0;579,8]	**535.7** [517.2;573.4]	**539.0** [517.2;556,9]
BW (g)	**23** [22;24,5]	**22** [21;26]	**24.5** [24;25,3]	**24** [22;25]	**23** [20.8;26]
IVS (mm)	**0.4** [0.4;0.5]	**0.4** [0.4;0.5]	**0.4** [0.4;0.4]	**0.5** [0.4;0.5][c]	**0.4** [0.4;0.5]
PW (mm)	**0.4** [0.3;0.4]	**0.4** [0.4;0.4]	**0.5** [0.4;0.5]	**0.4** [0.4;0.5]	**0.4** [0.4;0.45]
LVEDD (mm)	**3.4** [2.9;3.5]	**3.7** [3.45;3.8][a]	**3.2** [3.1;3.4]	**3.6** [3.4;3.95][e]	**3.4** [3.18;3.73]
LVESD (mm)	**2.0** [1.7;2.2]	**2.6** [2.3;2.9][b]	**1.9** [1.9;2]	**2.7** [2.4;3.1][e]	**2.3** [2.1;2.7][f]
LVM (mg)	**32.09** [26.63;43.75]	**44.80** [40.45;49.25][a]	**39.20** [31.22;42.49]	**46.95** [44.72;54.12][d]	**40.45** [37.78;45.33][g]
LVFS (%)	**41.311** [38,49;42.94]	**28.855** [24.32;33.77][b]	**40.901** [38.71;43.17]	**25.714** [20.55;29.18][e]	**32.258** [26.68;33.33][f]

BW, body weight; IVS, inter ventricular septum; PW, left ventricular posterior wall; LVEDD, left ventricular end diastolic diameter; LVESD, left ventricular end systolic diameter; LVM, left ventricular mass; LVFS, left ventricular fractional shortening; values are median [Q1;Q3].
P-value ≤ 0.05, [a]P-value ≤ 0.01 and [b]P-value ≤ 0.001: P-value obtained between WT and $Lmna^{H222P/H222P}$ (H222P) mice at 6 months of age using a two-sided Student t-test for heart rate and LVFS parameters and a two-sided Wilcoxon test for the others parameters.
P-value ≤ 0.05, [d]P-value ≤ 0.01 and [e]P-value ≤ 0.001: P-value obtained between WT and $Lmna^{H222P/H222P}$ (H222P vehicle-treated) mice at 7 months of age using a two-sided Student t-test for heart rate parameter and a two-sided Wilcoxon test for the others parameters.
[f] P-value ≤ 0.05, [g] P-value ≤ 0.01, ††† P-value ≤ 0.001: P-value obtained between NAC-treated and $Lmna^{H222P/H222P}$ (H222P vehicle-treated) mice at 7 months of age using a two-sided Student t-test for heart rate parameter and a two-sided Wilcoxon test for the others parameters.

In conclusion, our experiments demonstrate a novel contributory mechanism for *LMNA* cardiomyopathy triggered by oxidative stress and impaired antioxidant protection. Moreover, we have shown that NAC treatment restores GSH levels and reduces oxidative stress damage in the hearts of $Lmna^{H222P/H222P}$ mice. Because NAC pharmacodynamics and absence of toxicity

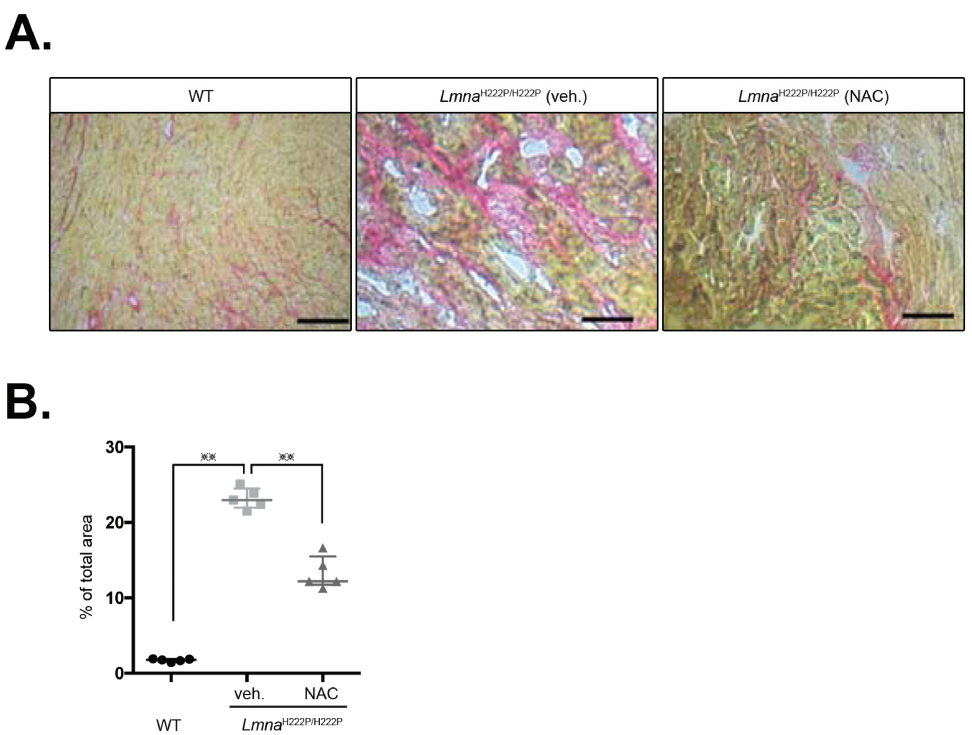

Figure 4. NAC improves myocardial fibrosis in *LMNA* cardiomyopathy. **(A)** Sirius Red staining of cross sections of the hearts from WT, vehicle-treated *Lmna*$^{H222P/H222P}$ (H222P) and NAC-treated *Lmna*$^{H222P/H222P}$ mice. Scale bar: 50 µm. **(B)** Heart fibrosis quantification from WT (n = 5), vehicle-treated *Lmna*$^{H222P/H222P}$ (H222P) (n = 5) and NAC-treated *Lmna*$^{H222P/H222P}$ mice (n = 5). For each mice, five cross-sections were quantified and the mean of the five cross-sections was represented and analyzed. Data are represented as median [Q1; Q3] ($^{¤¤}$*P*-value ≤ 0.01: *P*-value obtained using a Wilcoxon test on mean value of the five cross-sections).

are well established (28), our work supports further studies on humans to begin to evaluate the therapeutic benefits of lowering oxidative stress and assessing the benefit of such therapy in cardiomyopathy. Overall, our work points toward clinically relevant NAC as a possible future treatment option for patients with *LMNA* cardiomyopathy in addition to standard therapy.

Materials and Methods

Animals and experimental design

Experimental procedures were performed in accordance with European legislation on animal experimentation (L358-86/609/EEC). Homozygous knock-in mice carrying the *Lmna* p.H222P mutation (*Lmna*$^{H222P/H222P}$) were described previously (6). Six-month-old female *Lmna*$^{H222P/H222P}$ mice were given 1-month oral NAC (Merck; 140 mg/kg per day) in drinking water and compared to sex- and age-matched vehicle-treated *Lmna*$^{H222P/H222P}$ and WT mice. Animals were euthanized at 7 months of age to harvest samples.

Echocardiography

Transthoracic echocardiography was performed by an investigator unaware of the mouse genotype or treatment, with an Acuson 128XP/10 ultrasound system and a 10 MHz Acuson linear probe (Mountain View). Slight anesthesia of the mouse at room temperature with 0.5–1% isoflurane in O_2 (Abbott Inc.) was continuously adjusted to maintain heart rate.

Biochemical analyses

Detection of carbonylated proteins was performed from heart homogenates using Oxyblot protein oxidation detection kit (Chemicon International) based on immunochemical detection of protein carbonyl groups derivatized with 2,4-dinitrophenyl hydrazine. GSH was measured in heart homogenates and serum, according to a modification of Tietze method (29) as previously described (30,31).

RNA isolation and real-time polymerase chain reaction (PCR) analyses

Total RNA was extracted from frozen hearts using RNeasy Fibrous Tissue kit (QIAGEN). Concentration of total RNA was calculated using a NanoDrop ND-1000 spectrophotometer (Labtech), and RNA quality was assessed by electrophoresis. cDNA was synthesized using SuperScript III First-Strand Synthesis System for RT-PCR (Invitrogen). Mouse primer sequences used for transcriptional analyses were as follows: *mGclC* 5'-ATCCTCCAGTTCCTGCACAT-3', 5'-TGTGAATCCAGGGCCTA-3'; *mGsR* 5'-ACCACGAGGAAGACGAAATG-3', 5'-GGTGACCAGCTCCT CTGAAG-3'; *mNox2* 5'-GGCTGGGATGAATCTAGGCCAA-3', 5'-ACTGGTTTCCTGGTGAAAGAGCGG-3'. Real-time PCR was carried out on a Light Cycler (Roche Diagnostics), using the Quantitest SYBR green kit (QIAGEN) with sense and antisense oligonucleotides primers for the different genes. Relative levels of mRNA expression were calculated according to the ΔCT method (32).

Immunoblotting

Total proteins were isolated from mouse heart tissue in extraction buffer (Cell Signaling) with the addition of protease

inhibitors (25 mg/ml aprotinin, 10 mg/ml leupeptin, 1 mM 4-[2-aminoethyl]-benzene sulfonylfluoride hydrochloride and 2 mM Na_3VO_4). The lysates were sonicated (3 pulses of 10s at 30% amplitude) to allow dissociation of protein from chromatin and solubilization. Extracts were analyzed by sodium dodecyl sulfate–polyacrylamide gel electrophoresis (SDS-PAGE) using a 10% gel and transferred onto nitrocellulose membranes (Invitrogen). Subsequent to washes with Tris-buffered saline containing 1% Tween 20 (TBS-T), the membranes were blocked in 5% bovine serum albumin in TBS-T for 1 h at room temperature, then incubated with the appropriate antibody overnight at 4°C. The membranes were incubated with horseradish peroxidase-conjugated anti-rabbit or anti-mouse antibodies for 1 h at room temperature. After washing with TBS-T, the signal was revealed using Immobilon Western Chemiluminescent HorseRadish Peroxidase (HRP) Substrate (Millipore) on a G-Box system with GeneSnap software (Ozyme). Primary antibodies used were rabbit polyclonal antibodies that recognize NOX2 (Abcam), GPX1 (Cell Signaling) and GAPDH (Santa Cruz).

Histology

Hearts from mice were fixed in 4% formaldehyde for 48 h, embedded in paraffin, sectioned at 5 µm and stained with Sirius Red trichrome. Representative stained sections were photographed using a Microphot SA (Nikon) light microscope attached to a Spot RT Slide camera (Diagnostic Instruments). Images were processed using Adobe Photoshop CS (Adobe Systems).

Statistical analyses

For echocardiographic parameters, results were expressed as median [Q1;Q3]. The statistical analyses were performed by comparing the WT animals and *Lmna*$^{H222P/H222P}$ mice at baseline (6 months) and by comparing the WT mice to the vehicle-treated *Lmna*$^{H222P/H222P}$ mice post-treatment (7 months) and to evaluate the NAC treatment effect by comparing the vehicle-treated *Lmna*$^{H222P/H222P}$ mice and the NAC-treated *Lmna*$^{H222P/H222P}$ mice at 7 months. For each analysis a normality test was performed, followed by a Student t-test (for normally distributed data) or Wilcoxon test (for not normally distributed data). For echography parameters Student t-test was performed for the heart rate and LVFS parameters and a Wilcoxon test was performed for the other parameters. In order to have a better understanding of the LVFS % progression for each mice, we analyzed the ΔFS (ΔFS=7 months LVFS – 6 months LVFS), a Student t-test was performed.

For mRNA expression, statistical analysis was performed in ΔCt and the mRNA expression values normalized to the reference gene was graphically represented. The results are presented as mean±SEM. In the GSH concentration (serum and heart) and fibrosis parameter, results were expressed as median [Q1;Q3]. The statistical analyses were performed by comparing the WT animals and the vehicle-treated *Lmna*$^{H222P/H222P}$ mice and to evaluate the NAC treatment effect by comparing the vehicle-treated *Lmna*$^{H222P/H222P}$ mice and the NAC-treated *Lmna*$^{H222P/H222P}$ mice. For both analyses, a Student t-test was performed for the mRNA expression and GSH concentration (heart) parameters and a Wilcoxon test was performed for GSH concentration (serum) and fibrosis parameter.

The significance level is taken to 5%. Statistical analyses were conducted using SAS 9.2 (SAS Institute Inc., USA).

Acknowledgements

Authors thank Christelle Enond, technical head of the Nouvelle Animalerie Commune at the Medecine Department of UPMC University Paris 06 and animal facility personnel for the *Lmna* mouse line breeding.

Conflict of Interest statement. Blanca Morales Rodriguez is employed by Sanofi, a global biopharmaceutical company focused on human health.

Funding

Agence Nationale de la Recherche (ANR)-Gis Maladies Rares (#ANR-05-MRAR-035); Association Française contre les Myopathies, the European Union Sixth Framework Programme (Eurolaminopathies #018690); the Program for Promotion of Fundamental Studies in Health Sciences of the National Institute of Biomedical Innovation (NIBIO, Japan); Sanofi (through a CIFRE PhD grant to B.M.R.).

References

1. Bonne, G., Di Barletta, M.R., Varnous, S., Bécane, H.M., Hammouda, E.H., Merlini, L., Muntoni, F., Greenberg, C.R., Gary, F., Urtizberea, J.A., *et al.* (1999) Mutations in the gene encoding lamin A/C cause autosomal dominant Emery–Dreifuss muscular dystrophy. *Nat. Genet.*, **21**, 285–288.
2. Fatkin, D., MacRae, C., Sasaki, T., Wolff, M.R., Porcu, M., Frenneaux, M., Atherton, J., Vidaillet, H.J., Spudich, S., De Girolami, U., *et al.* (1999) Missense mutations in the rod domain of the lamin A/C gene as causes of dilated cardiomyopathy and conduction-system disease. *N. Engl. J. Med.*, **341**, 1715–1724.
3. Meune, C., Van Berlo, J.H., Anselme, F., Bonne, G., Pinto, Y.M. and Duboc, D. (2006) Primary prevention of sudden death in patients with lamin A/C gene mutations. *N. Engl. J. Med.*, **354**, 209–210.
4. Ben Yaou, R., Gueneau, L., Demay, L., Stora, S., Chikhaoui, K., Richard, P. and Bonne, G. (2006) Heart involvement in lamin A/C related diseases. *Arch. Mal. Coeur Vaiss.*, **99**, 848–855.
5. Lu, J.T., Muchir, A., Nagy, P.L. and Worman, H.J. (2011) LMNA cardiomyopathy: cell biology and genetics meet clinical medicine. *Dis. Model. Mech.*, **4**, 562–568.
6. Arimura, T., Helbling-Leclerc, A., Massart, C., Varnous, S., Niel, F., Lacène, E., Fromes, Y., Toussaint, M., Mura, A.M., Keller, D.I., *et al.* (2005) Mouse model carrying H222P-Lmna mutation develops muscular dystrophyand dilated cardiomyopathy similar to human striated muscle laminopathies. *Hum. Mol. Genet.*, **14**, 155–169.
7. Muchir, A., Pavlidis, P., Decostre, V., Herron, A.J., Arimura, T., Bonne, G. and Worman, H.J. (2007) Activation of MAPK pathway links LMNA mutations to cardiomyopathy in Emery–Dreifuss muscular dystrophy. *J. Clin. Invest.*, **117**, 282–1293.
8. Muchir, A., Wu, W., Choi, J.C., Iwata, S., Morrow, J.P., Homma, S. and Worman, H.J. (2012) Abnormal p38a mitogen activated protein kinase signalling in dilated cardiomyopathy caused by lamin A/C gene mutation. *Hum. Mol. Genet.*, **21**, 4325–4333.
9. Le Dour, C., Macquart, C., Sera, F., Shunichi, H., Bonne, G., Morrow, J.P., Worman, H.J. and Muchir, A. (2017) Decreased WNT/b-catenin signalling contributes to the pathogenesis of dilated cardiomyopathy caused by mutations in the lamin A/C gene. *Hum. Mol. Genet.*, **26**, 333–343.

10. Chatzifrangkeskou, M., Le Dour, C., Wu, W., Morrow, J.P., Joseph, L.C., Beuvin, M., Sera, F., Homma, S., Vignier, N., Mougenot, N. *et al.* (2016) ERK1/2 directly acts on CTGF/CCN2 expression to mediate myocardiacl fibrosis in cardiomyopathy caused by mutation in the lamin A/C gene. *Hum. Mol. Genet.*, **25**, 2220–2233.
11. Choi, J.C., Muchir, A., Wu, W., Iwata, S., Homma, S., Morrow, J.P. and Worman, H.J. (2012) Temsirolimus activates autophagy and ameliorates cardiomyopathy caused by lamin A/C gene mutation. *Sci. Transl. Med.*, **4**, 144ra102.
12. Arimura, T., Sato, R., Machida, N., Bando, H., Zhan, D.Y., Morimoto, S., Tanaka, R., Yamane, Y., Bonne, G. and Kimura, A. (2010) Improvement of left ventricular dysfunction and of survival prognosis of dilated cardiomyopathy by administration of calcium sensitizer SCH00013 in a mouse model. *J. Am. Coll. Cardiol.*, **55**, 1503–1505.
13. Worman, H.J. (2018) Cell signaling abnormalities in cardiomyopathy caused by lamin A/C gene mutations. *Biochem. Soc. Trans.*, **46,** 37–42.
14. Sieprath, T., Darwiche, R., and De Vos, W.H. (2012) Lamins as mediators of oxidative stress. *Bioch. Biophys. Res. Comm.*, **421**, 635–639.
15. Schieber, M. and Chandel, N.S. (2014) ROS function in redox signaling and oxidative stress. *Curr. Biol.*, **24**, 453–462.
16. Bonne, G., Mercuri, E., Muchir, A., Urtizberea, A., Bécane, H.M., Recan, D., Merlini, L., Wehnert, M., Boor, R., Reuner, U., *et al.* (2000) Clinical and molecular genetic spectrum of autosomal dominant Emery–Dreifuss muscular dystrophy due to mutations of the lamin A/C gene. *Ann. Neurol.*, **48**, 170–180.
17. Caron, M., Auclair, M., Donadille, B., Béréziat, V., Guerci, B., Laville, M., Narbonne, H., Bodemer, C., Lascols, O., Capeau, J. *et al.* (2007) Human lipodystrophies linked to mutations in A-type lamins and to HIV protease inhibitor therapy are both associated with prelamin A accumulation, oxidative stress and premature cellular senescence. *Cell Death Differ.*, **14**, 1759–1767.
18. Charniot, J.C., Bonnefont-Rousselot, D., Marchand, C., Zerhouni, K., Vignat, N., Peynet, J., Plotkine, M., Legrand, A. and Artigou, J.Y. (2007) Oxidative stress implication in a new phenotype of amyotrophic quadricipital syndrome with cardiac involvement due to lamin A/C mutation. *Free Radic. Res.*, **41**, 424–431.
19. Tsutsui, H., Kinugawa, S. and Matsushima, S. (2011) Oxidative stress and heart failure. *Am. J. Physiol. Heart Circ. Physiol.*, **301**, H2181–H2190.
20. Nordberg, J. and Arner, E.S.J. (2001) Reactive oxygen species, antioxidants, and the mammalian thioredoxin system. *Free Radic. Biol. Med.*, **31**, 1287–1312.
21. Marian, J., Senthil, V., Chen, S.N. *et al.* (2006) Antifibrotic effects of antioxidant N-acetylcysteine in a mouse model of human hypertrophic cardiomyopathy mutation. *J. Am. Coll. Cardiol.*, **47**, 827–834.
22. Kono, Y., Nakamura, K., Kimura, H., Nishii, N., Watanabe, A., Banba, K., Miura, A., Nagase, S., Sakuragi, S., Kusano, K.F., Matsubara, H. *et al.* (2006) Elevated levels of oxidative DNA damage in serum and myocardium of patients with heart failure. *Circ. J.*, **70**, 1001–1005.
23. Gopal, D.M. and Sam, F. (2013) New and emerging biomarkers in left ventricular systolic dysfunction-insight into dilated cardiomyopathy. *J. Cardiovasc. Transl. Res.*, **6**, 516–527.
24. Farías, J.G., Molina, V.M., Carrasco, R.A., Zepeda, A.B., Figueroa, E., Letelier, P. and Castillo, R.L. (2017). Antioxidant therapeutic strategies for cardiovascular conditions associated with oxidative stress. *Nutrients*, **9**, pii:E966. doi:10.3390/nu9090966
25. Richards, S.A., Muter, J., Ritchie, P., Lattanzi, G. and Hutchison, C.J. (2011) The accumulation of un-repairable DNA damage in laminopathy progeria fibroblasts is caused by ROS generation and is prevented by treatment with N-acetyl cysteine. *Hum. Mol. Genet.*, **20**, 3997–4004.
26. Pekovic, V., Gibbs-Seymour, I., Markiewicz, E., Alzoghaibi, F., Benham, A.M., Edwards, R., Wenhert, M., von Zglinicki, T. and Hutchison, C.J. (2011) Conserved cysteine residues in the mammalian lamin A tail are essential for cellular responses to ROS generation. *Aging Cell*, **10**, 1067–1079.
27. Singh, M., Hunt, C.R., Pandita, R.K., Kumar, R., Yang, C.R., Horikoshi, N., Bachoo, R., Serag, S., Story, M.D., Shay, J.W. *et al.* (2013) Lamin A/C depletion enhances DNA damage-induced stalled replication fork arrest. *Mol. Cell Biol.*, **33**, 1210–1222.
28. Pendyala, F. and Creaven, P.J. (1995) Pharmacokinetic and pharmacodynamic studies of N-acetylcysteine, a potential chemopreventive agent during a phase I trial. *Cancer Epidemiol Biomarkers Prev.*, **4**, 245–251.
29. Tietze, F. (1969) Enzymic method for quantitative determination of nanogram amounts of total and oxidized glutathione: applications to mammalian blood and other tissues. *Anal. Biochem.*, **27**, 502–522.
30. Adamy, C., Mulder, P., Khouzami, L., Andrieu-abadie, N., Defer, N., Candiani, G., Pavoine, C., Caramelle, P., Souktani, R., Le Corvoisier, P., Perier, M. *et al.* (2007) Neutral sphingomyelinase inhibition participates to the benefits of N-acetylcysteine treatment in post-myocardial infarction failing heart rats. *J. Mol. Cell. Cardiol.*, **43**, 344–353.
31. Rahman, I., Kode, A. and Biswas, S.K. (2006) Assay for quantitative determination of glutathione and glutathione disulfide levels using enzymatic recycling method. *Nat. Protoc.*, **1**, 3159–3165.
32. Ponchel, F., Toomes, C., Bransfield, K., Leong, F.T., Douglas, S.H., Field, S.L., Bell, S.M., Combaret, V., Puisieux, A., Mighell, A.J. *et al.* (2003) Real-time PCR based on SYBR-Green I fluorescence: an alternative to the TaqMan assay for a relative quantification of gene rearrangements, gene amplifications and micro gene deletions. *BMC Biotechnol.*, **3**, 18.